Mixed Phosphine/Carbonyl Derivatives of Heterobimetallic Copper-Iron and Copper-Tungsten Catalysts

Noel J. Leon[†], Hsien-Cheng Yu[†], Thomas J. Mazzacano, Neal P. Mankad*

Department of Chemistry, University of Illinois at Chicago, 845 W. Taylor St., Chicago, IL 60607, USA
*Corresponding author: npm@uic.edu
[†]These authors contributed equally

Abstract: Evolution of dihydrogen was observed from reactions of protic metal-hydride complexes $FeCp(CO)(PR_3)H$ and $WCp^*(CO)_2(PR_3)H$ with hydridic (NHC)CuH complexes, providing access to several heterobimetallic (NHC)Cu-$FeCp(CO)(PR_3)$ and (NHC)Cu-$WCp^*(CO)_2(PR_3)$ complexes that are the mixed phosphine/carbonyl derivatives of previously studied catalysts for C-H borylation (NHC = *N*-heterocyclic carbene). The new complexes were characterized by multinuclear NMR spectroscopy, FT-IR spectroscopy, and in some cases X-ray crystallography. In one case, a (NHC)Cu$(\mu_2\text{-H})_2$FeCp(PPh_3) complex was structurally characterized as the decomposition product of an unstable (NHC)Cu-$FeCp(CO)(PPh_3)$ derivative. Preliminary trials in C-H borylation catalysis are reported, including measurable activity under photochemical conditions.

Graphical abstract:

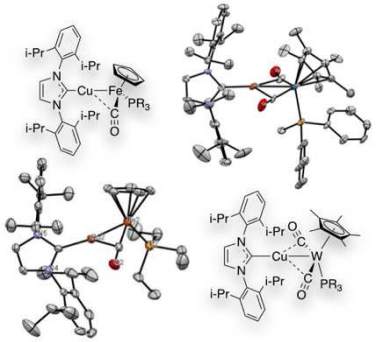

Synopsis: Heterobimetallic Cu-Fe and Cu-W complexes with mixed phosphine/ligation were synthesized, characterized, and test in C-H borylation catalysis.

Keywords: heterobimetallic, borylation, copper, iron, tungsten, hydride

Supplementary material: Supplementary material (spectral data) is enclosed. Crystallographic files are available from the Cambridge Structural Database (CCDC 1860130-1860135)

Introduction

Construction of complex organic scaffolds from simpler building blocks generally relies on the presence of reactive heteroatom functional groups or unsaturated bonds. Using ubiquitous C-H positions directly in coupling reactions is comparatively desirable because it greatly reduces the number of synthetic steps by circumventing the need for pre-installed functionalities.[1–6] However, the thermodynamic stability and kinetic inertness of C-H bonds present great challenges to be overcome, as does the problem of site selectivity in organic substrates containing multiple distinct C-H sites. In this regard, transition metal-catalyzed C-H borylation is one of the most promising technologies to emerge recently.[7,8] In this transformation, C-H bonds are converted directly to organoboronic esters that, in turn, can be used in the Suzuki-Miyaura reaction or translated into a plethora of other functional groups.[9] Crucially, the C-H borylation reaction obeys well-defined site-selectivity rules guided primarily by C-H acidity or steric accessibility, and catalysts have been developed that facilitate mild reaction conditions. These qualities are best displayed with C-H borylation catalysts based on the precious metal, Ir, ligated by diphosphine, bipyridine, and pincer systems. Recent advances have been made with catalytic C-H borylation using non-precious metals such as Fe,[10–12] Ni,[13] and Co,[14–18] as well as with a metal-free strategy employing frustrated Lewis pairs.[19] While promising, these non-precious metal systems typically exhibit efficient reactivity only for highly activated and/or acidic C-H bonds and require solvent quantities of substrate in order for borylation of unactivated C-H bonds to occur. Thus, more work is required to access non-precious metal catalysts for efficient borylation of unactivated C-H bonds in stoichiometric quantities.

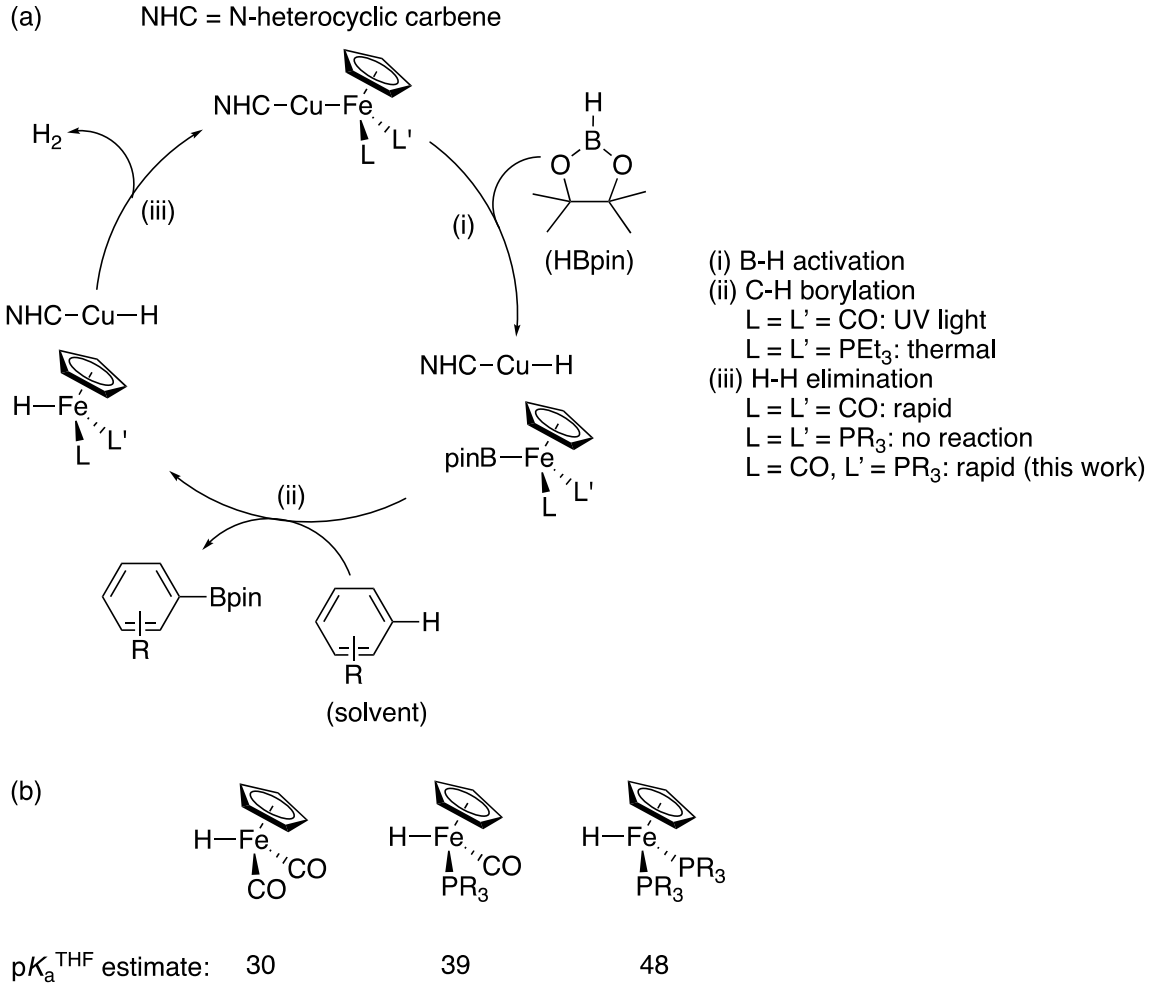

Scheme 1. (a) Summary of heterobimetallic C-H borylation catalysis; (b) Estimates of [Fe]-H pK_a values in THF based on ligand acidity constants.[20] A similar scheme is operative for (NHC)Cu-WCp*$(CO)_2$L analogues (L = CO or PR_3).

A long term goal of our research group is to use the cooperative behavior of heterobimetallic catalysts to uncover catalytic transformations with non-precious metals that complement single-site precious metal systems.[21–23] One of our first forays into this area involved the discovery that (IPr)Cu-FeCp$(CO)_2$,[24] and later (IPr)Cu-WCp*$(CO)_3$,[25] are active catalysts for borylation of arene solvents upon exposure to UV light with a 450-W Hg lamp over 24h (IPr = *N*,*N*'-bis(2,6-diisopropylphenyl)imidazol-2-ylidene). These systems rely on the known stoichiometric borylation activity of FeCp$(CO)_2$B$(OR)_2$ and WCp*$(CO)_3$B$(OR)_2$ intermediates under UV irradiation conditions that was studied in detail by Hartwig many years ago (Scheme 1a, step ii).[26–28] In our heterobimetallic system, the copper-carbene unit acts as a hydride shuttle that allows for the active Fe- or W-based borylating agents to be continuously regenerated catalytically via cooperative heterobimetallic B-H activation and H-H elimination reactions that occur thermally (Scheme 1a, steps i and iii).[29] Because the C-H borylation step (Scheme 1a, step ii) is known to involve photochemical CO dissociation,[30] we have been targeting a thermal C-H borylation catalyst by replacing one or more CO ligands with labile phosphines.[31] We were able to demonstrate that FeCp$(PEt_3)_2$Bpin mediates stoichmetric, UV-free borylation of arene solvents at 70-80°C due to thermal PEt_3 lability from this sterically

crowded complex, but catalysis was precluded because heterobimetallic H-H elimination from (IPr)CuH + $FeCp(PEt_3)_2H$ (Scheme 1a, step iii) did not occur readily.[32] Our hypothesis is that this H-H elimination step requires a highly polarized system where a hydridic [Cu]-H species reacts with a protic [Fe]-H species.[33] Indeed, while $FeCp(CO)_2H$ is known to be significantly protic in character, the $FeCp(PEt_3)_2H$ analogue is less acidic by ~19 pK_a units (Scheme 1b).[20] This has led us to target mixed phosphine/carbonyl catalysts of the type (NHC)Cu-$FeCp(CO)(PR_3)$, which we hope will mediate thermal C-H borylation while facilitating catalytic turnover via $FeCp(CO)(PR_3)H$ intermediates with more protic character (Scheme 1b). Synthesis and characterization of such mixed phosphine/carbonyl catalysts are reported in this manuscript, as is the demonstration that heterobimetallic H-H elimination does indeed proceed as expected when at least one carbonyl ligand is present in the system.

Results and discussion

The iron hydride complexes $FeCp(CO)(PR_3)H$ were observed to react rapidly within 5 minutes with *in situ*-generated (IPr)CuH to release H_2 and provide (IPr)Cu-$FeCp(CO)(PR_3)$ complexes (**1a-d**, Scheme 2). In typical reactions, the crude product mixtures contained a minor side-product tentatively identified as CpFe(IPr)(CO)H (hydride signal: -17.35 ppm) by comparison to the Ru analogue,[33] and complexes **1a-d** could be isolated in 21-44% recrystallized yield. Not only does this dehydrogenation reaction provide a synthetic method for these new mixed phosphine/carbonyl heterobimetallic complexes, but it provides further indication that the catalytically relevant H_2 elimination step (Scheme 1, step iii) is viable if the [Fe]-H pK_a is low enough. Complexes **1a-d** were characterized by multinuclear NMR spectroscopy and FT-IR spectroscopy. X-ray crystallography data was obtained for complexes **1b** and **1d**. Vibrational data for the carbonyl ligands and selected bond metrics are shown in Table 1 for comparison to (IPr)Cu-$FeCp(CO)_2$,[34,35] and solid-state structures are depicted in Figure 1. Unlike the thermally stable (IPr)Cu-$FeCp(CO)_2$ derivative, the mixed phosphine/carbonyl derivatives **1a-d** decompose at a measurable rate (2-12 hours at room temperature, see Supplementary Material), which we expect will limit their utility as catalysts.

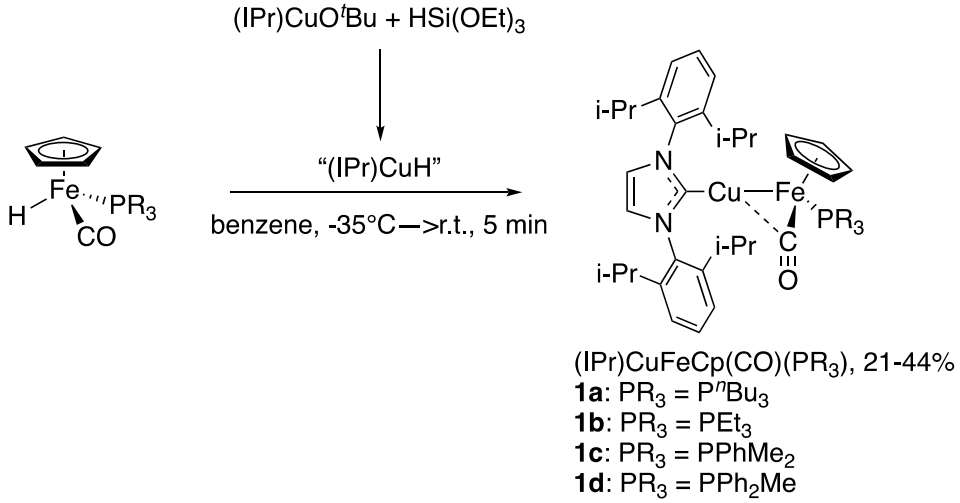

(IPr)CuFeCp(CO)(PR$_3$), 21-44%
1a: PR$_3$ = P^{n}Bu$_3$
1b: PR$_3$ = PEt$_3$
1c: PR$_3$ = PPhMe$_2$
1d: PR$_3$ = PPh$_2$Me

Scheme 2. Synthesis of mixed phosphine/carbonyl Cu-Fe heterobimetallic complexes.

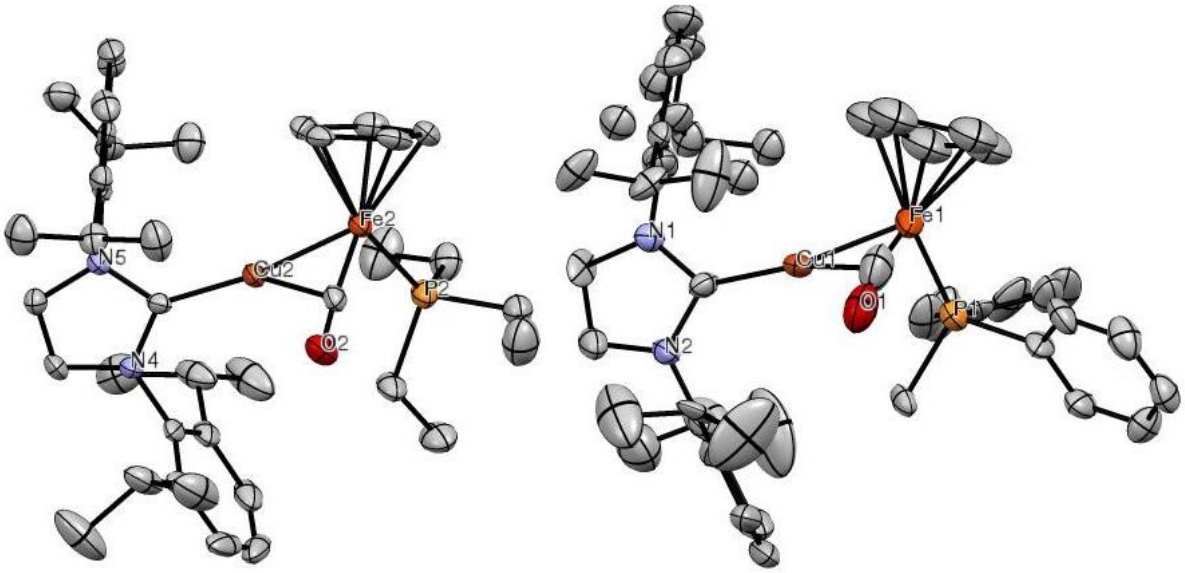

Figure 1. X-ray crystal structures of **1b** and **1d**, with ellipsoids shown at the 50% probability level. Hydrogen atoms and co-crystallized solvent molecules have been omitted, and only one of two independent molecules in the asymmetric unit of **1b** is shown. Selected bond metrics are given in Table 1.

Table 1. Selected data comparisons for Cu-Fe heterobimetallic complexes

Complex	ν_{CO} (cm^{-1})	*d*(Cu-Fe) (Å) / FSR[a]	*d*(Cu···CO) (Å)	*d*(C-O) (Å)	$\angle C_{NHC}$-Cu-Fe (°)	∠Fe-C-O (°)
(IPr)Cu-FeCp(CO)$_2$[b]	1914, 1849	2.3462(5) / 1.004	2.423(3), 2.749(3)	1.169(3)	170.16(7)	177.2(2)
(IPr)Cu-FeCp(CO)(P^{n}Bu$_3$) (**1a**)	1795	n.d.[c]	n.d.[c]	n.d.[c]	n.d.[c]	n.d.[c]
(IPr)Cu-FeCp(CO)(PEt$_3$) (**1b**)[d]	1791	2.3331(9) / 0.998	2.378(5)	1.186(6)	169.21(14)	176.5(4)
(IPr)Cu-FeCp(CO)(PPhMe$_2$) (**1c**)	1794	n.d.[c]	n.d.[c]	n.d.[c]	n.d.[c]	n.d.[c]
(IPr)Cu-FeCp(CO)(PPh$_2$Me) (**1d**)[e]	1813	2.299(2) / 0.983	2.440(18)	1.13(2)	170.2(15)	170.2(15)

[a]FSR = formal shortness ratio.[36] [b]Data from literature references.[34,35] [c]n.d. = not determined. [d]Structural data is given for one of two independent molecules in the asymmetric unit of **1b**. [e]R value is 0.34, so the reader should take caution in interpreting metrical parameters.

The accumulated data indicate, as expected, that phosphine ligation renders the Fe centers more electron-rich than in the parent (IPr)Cu-FeCp(CO)$_2$ derivative. This is particularly evident by examination of the carbonyl stretching frequencies for complexes **1a-d**, which are in the 1791-1813 cm^{-1} range and shifted to significantly lower energy than those of (IPr)Cu-FeCp(CO)$_2$ (Table 1). Both **1b** and **1d** feature semibridging carbonyl ligands,[37] which is indicated by van der Waals Cu$\cdots$C$_{CO}$ contact and confirmed by tabulation of Curtis's α parameter being 0.39 in both cases and thus in between the bridging CO ($\alpha \leq 0.1$) and terminal CO ($\alpha \geq 0.6$) regimes.[38] The impact on metal-metal bonding of the increased electron density at Fe is a slight contraction of the Cu-Fe distance. Based on our model from previous spectroscopic and computational studies,[39] we propose that the modestly shortened Cu-Fe distances in **1b** and **1d** result from enhanced donation in the Fe$\rightarrow$Cu dative bond. No significant deviations in C$_{NHC}$–Cu–Fe angle were observed, indicating that a single phosphine ligand does not provide sufficient steric pressure to strain the metal-metal bond.

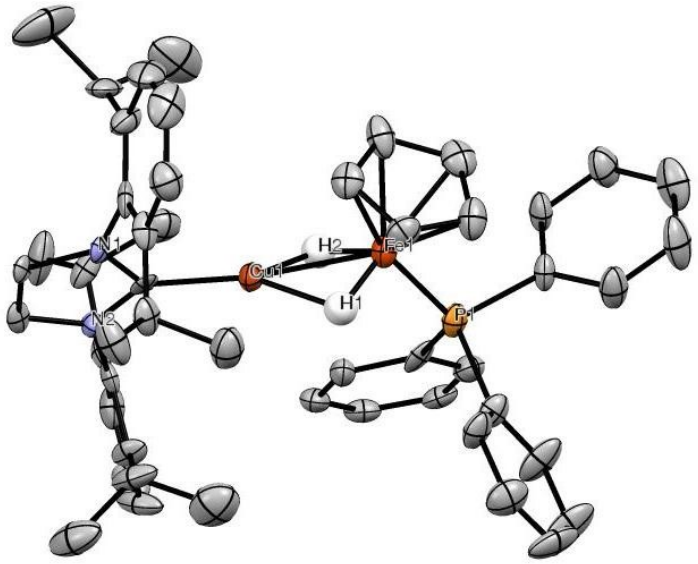

Figure 2. X-ray crystal structure of **2**, with ellipsoids shown at the 50% probability level. C-H hydrogens are omitted. H1 and H2 were located in the Fourier difference map and refined isotropically. Selected distances (Å): Cu1-Fe1, 2.3652(16); Cu1-H1, 1.76(5); Cu1-H2, 1.68(4); Fe1-H1, 1.39(6); Fe1-H2, 1.70(6); H1-H2, 2.0(1).

When our synthetic method was used to target (IPr)Cu-FeCp(CO)(PPh$_3$) (**1e**), we did observe a ^{31}P NMR resonance at 89.6 ppm, consistent with initial formation of **1e** by comparison to analogues **1a-d**. However, **1e** appears to be unstable. When we tried to recrystallize **1e**, we only obtained a small amount of crystals of a decomposition product, whose ^{31}P NMR signal was shifted to 94.7 ppm and which was identified as (IPr)Cu(μ-H)$_2$FeCp(PPh$_3$) (**2**, Figure 2) by X-ray crystallography. We have been unable to synthesize **2** independently or isolate it in large enough quantities for full characterization and reactivity studies. We assume that source of hydrogen during decomposition is the side-product contaminant CpFe(IPr)(CO)H, which was observed in the crude mixture by ^{1}H NMR. A related complex LCu(μ_2-H)$_2$WCp$_2$ (L = β-diketiminate) was reported recently by Crimmin, who formulated its bonding as consisting of a σ-adduct of H$_2$WCp$_2$ bound to [LCu] through η^2:η^2-binding of two W-H σ-bonds to Cu(I).[40] By analogy, one view of **2** is as a η^2:η^2-adduct of anionic [H$_2$FeCp(PPh$_3$)]$^-$ to cationic [(IPr)Cu]$^+$. However,

we cannot rule out an alternative representation of heterodinuclear **2** as the η^2-adduct of neutral [HFeCp(PPh_3)] bound to neutral [(IPr)CuH]. The H···H distance in **2** of 2.0(1) Å is clearly too long to invoke any dihydrogen interaction.[41][42]

Related chemistry is available for the tungsten analogues. Slow dihydrogen evolution occurred from the reaction of WCp*$(CO)_2(PR_3)$H complexes with either (IPr)CuH or (6Pr)CuH (6Pr = *N*,*N*'-bis(2,6-diisopropylphenyl)-4,5,6,7-tetrahydro-1,3-diazepin-2-ylidene), providing heterobimetallic (NHC)Cu-WCp*$(CO)_2(PR_3)$ complexes in 15-66% yield (**3a-d**, Scheme 3). The observed reactivity is consistent with the estimated pK_a^{THF} values of 14 for WCp*$(CO)_2(PR_3)$H.[43] These complexes were characterized by multinuclear NMR spectroscopy and FT-IR spectroscopy, and derivatives **3b-d** were characterized by X-ray crystallography. Relevant data is shown in Table 2 for comparison to (IPr)Cu-WCp$(CO)_3$, and solid-state structures for **3b-c** are depicted in Figure 3. Unlike iron analogues **1a-d**, the tungsten complexes **3a-d** are quite robust thermally and do not decompose upon prolonged heating at 67°C.

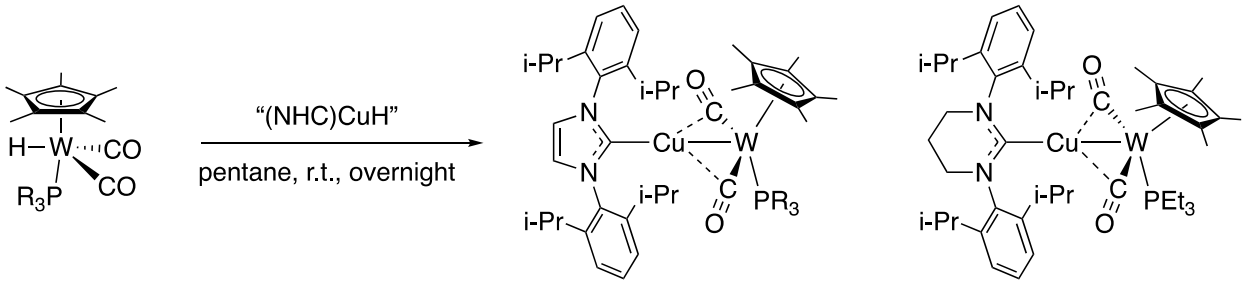

(IPr)CuWCp*$(CO)_2(PR_3)$, 44-66%
3a: PR_3 = PEt_3
3b: PR_3 = $PPhMe_2$
3c: PR_3 = PPh_2Me

(6Pr)CuWCp*$(CO)_2(PEt_3)$ 9% (**3d**)

Scheme 3. Synthesis of mixed phosphine/carbonyl Cu-W heterobimetallic complexes.

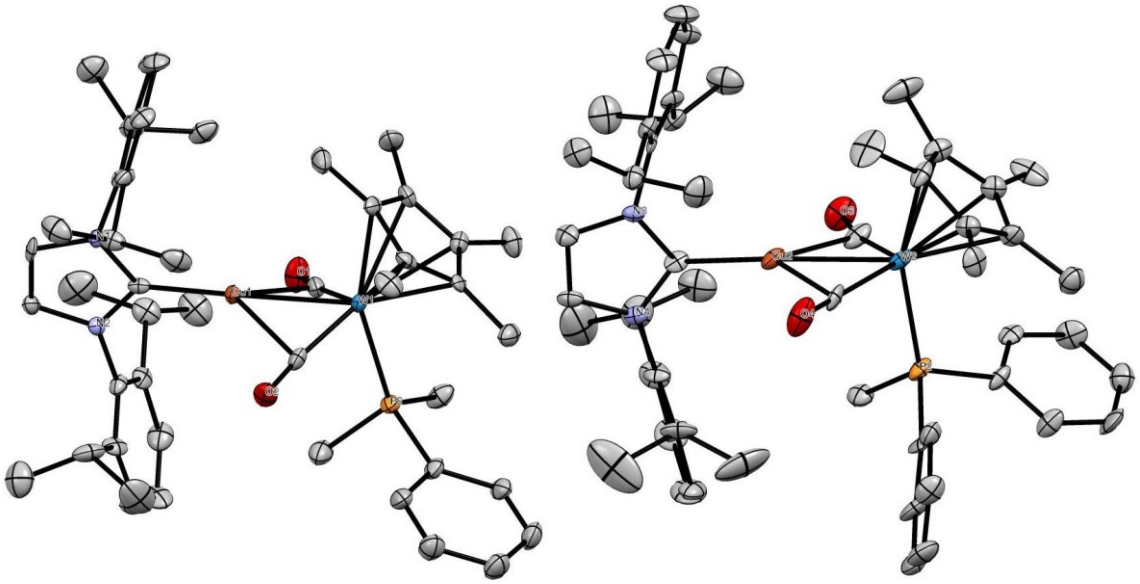

Figure 3. X-ray crystal structures of **3b** and **3c**, with ellipsoids shown at the 50% probability level. Hydrogen atoms have been omitted, and only one of two independent molecules in the asymmetric unit of **3c** is shown. Selected bond metrics are given in Table 2.

Table 2. Selected data comparisons for Cu-W heterobimetallic complexes

Complex	ν_{CO} (cm^{-1})	*d*(Cu-W) (Å) / FSR[a]	*d*(Cu···CO) (Å)	*d*(C-O) (Å)	$\angle C_{NHC}$-Cu-W (°)	∠W-C-O (°)
(IPr)Cu-WCp(CO)$_3$[b,c]	1920, 1818, 1784	2.5599(6) / 1.035	2.294(7), 2.280(5), 3.858(6)	1.174(8), 1.16(1), 1.159(7)	165.7(1)	173.5(5)
(IPr)Cu-WCp*(CO)$_2$(PEt$_3$) (**3a**)	1750, 1691	n.d.[d]	n.d.[d]	n.d.[d]	n.d.[d]	n.d.[d]
(IPr)Cu-WCp*(CO)$_2$(PPhMe$_2$) (**3b**)	1778, 1702	2.5490(8) / 1.031	2.205(2), 2.227(2)	1.197(2), 1.204(2)	178.02(5)	171.6(1), 172.1(1)
(IPr)Cu-WCp*(CO)$_2$(PPh$_2$Me) (**3c**)[c]	1762, 1693	2.579(1) / 1.043	2.15(1), 2.18(1)	1.17(2), 1.19(2)	178.8(3)	167.6(9), 168(1)
(6Pr)Cu-WCp*(CO)$_2$(PEt$_3$) (**3d**)	1753, 1688	2.6137(5) / 1.057	2.2022(7), 2.2143(7)	1.1801(7), 1.1849(8)	177.37(3)	168.58(5), 170.60(5)

[a]FSR = formal shortness ratio.[36] [b]Data from literature references.[35] [c]Structural data is given for one of two independent molecules in the asymmetric units of (IPr)CuWCp(CO)$_3$ and **3c**. [d]n.d. = not determined.

The overall trends for the Cu-W series are similar to those noted above for the Cu-Fe series. The W center is, as expected, more electron-rich upon phosphine ligation in **3a-d**, whose

carbonyl stretching frequencies are shifted to lower energies from the corresponding features in (IPr)Cu-WCp(CO)$_3$ (Table 2). Both **3b** and **3d** feature a pair of semibridging carbonyl ligands according to their α parameters of ~0.13-0.15. Complex **3c** has one semibridging carbonyl ligand (α = 0.14) and one carbonyl ligand that borders on fully bridging (α = 0.10). The metal-metal bonding appears not to be impacted significantly by phosphine ligation, as the Cu-W distances in **3b-d** are all very similar to that of (IPr)Cu-WCp(CO)$_3$, with no clear trend emerging. This observation is consistent with greater delocalization of extra electron density at W into *two* carbonyls rather than one for Fe, thus providing very little available electron density for increased donation in the W→Cu dative bond. Once again, no evidence for steric pressure is observed structurally, as the C_{NHC}-Cu-W angles remain linear regardless of the ligands bound to W.

Due to their higher thermal stability the copper-tungsten complexes were pursued for C-H borylation catalysis in favor of the copper-iron analogues. Under UV irradiation conditions, complexes **3b-d** exhibited some activity for catalyzing borylation of benzene-d_6 solvent with pinacolborane (HBpin). However, the photochemical activity for **3b-d** was very poor (e.g., 27% conversion to C_6D_5Bpin with 20 mol% **3c** under UV irradiation with 450-W Hg lamp over 24 h at room temperature) compared to that observed for the parent (IPr)CuWCp*(CO)$_3$ (80% conversion to C_6D_5Bpin under identical conditions with 10 mol% (IPr)CuWCp*). [25] Even the modest photochemical C-H borylation activity with the mixed phosphine/carbonyl catalysts indicates that they are capable of performing the thermal B-H cleavage and H-H elimination reactions required for catalysis (Scheme 1, steps i and iii), and also that they furnish WCp*(CO)$_2$(PR$_3$)Bpin intermediates that are active for arene borylation when provided enough energy to induce ligand dissociation. Unfortunately, under UV-free conditions, no evidence for any catalytic activity was observed for borylation of arene solvents at temperatures up to 110°C. While disappointing, this lack of thermally-induced catalytic activity is consistent with the structural data discussed above. Specifically, the putative WCp*(CO)$_2$(PR$_3$)Bpin intermediates accessed from catalysts **3b-d** are presumably not sterically crowded enough for the phosphine ligand to be labile, and so the C-H functionalization step (Scheme 1, step ii) is inhibited. Attempts at synthesizing bulkier catalysts such as (IPr)Cu-WCp*(CO)$_2$(PPh$_3$) and (IPr)Cu-WCp*(CO)$_2$(PCy$_3$) failed, possibly due to instability imparted by overcrowding.

Conclusions

In conclusion, complexes with mixed phosphine/carbonyl ligation provide metal-hydride intermediates with sufficiently low pK_a values that they are capable of engaging in heterobimetallic H_2 evolution with a hydridic (NHC)CuH partner. Using this H_2 evolution reaction as a synthetic method, several (NHC)Cu-FeCp(CO)(PR$_3$) and (NHC)Cu-WCp*(CO)$_2$(PR$_3$) complexes were synthesized and thoroughly characterized. In one case, a (NHC)Cu-FeCp(PPh$_3$) complex was found to decay to yield an interesting (NHC)Cu(μ_2-H)$_2$FeCp(PPh$_3$) decomposition product. While the new copper-tungsten heterobimetallic complexes are active for photochemical C-H borylation, further work is needed to identify complexes with the right steric/electronic balance for thermally-induced catalysis.

Materials and methods

General Remarks. Unless otherwise noted, all the syntheses were done in a glovebox filled with N_2 or using standard Schlenk line techniques. Glassware was oven-dried prior to use. All the chemicals purchased from commercial vendors were used without further purification. Solvents were dried using a Glass Contour solvent purification system built by Pure Process Technology, LLC. Deuterated solvents that were packed under Ar were stored over 3-Å molecular sieves and used without further manipulation. Photolysis was conducted using a 450-W Hanovia mercury arc lamp in an immersion well filled with circulating water. (IPr)CuO^{t}Bu[44], [(IPr)CuH]$_2$[44], and (6Pr)CuH[45] were synthesized using previously published literature methods. CpFeCO(PR$_3$)I[46], CpFeCO(PR$_3$)H (R= PEt$_3$, P^{n}Bu$_3$, PMe$_2$Ph, PMePh$_2$, PPh$_3$)[25], and Cp*W(CO)$_2$(PR$_3$)H (R= PEt$_3$, PMe$_2$Ph, PMePh$_2$)[47], were all synthesized by adapted literature methods.

Instrumentation. All the NMR spectra were recorded at ambient temperature using either Bruker Avance DPX-400 or Bruker Avance DPX-500 MHz instruments. Mass analyses were performed with an Advion Expression^L CMS mass spectrometer using atmospheric pressure chemical ionization (APCI) in selected ion monitoring (SIM) mode. FT-IR spectra were recorded in a glovebox on powder samples using a Bruker ALPHA spectrometer fitted with a diamond-ATR detection unit. Elemental analyses were performed by the Midwest Microlab, LLC, in Indianapolis, IN. Single-crystal X-ray diffraction experiments were performed using a Bruker PHOTON II diffractometer. Data reduction, solution, and refinement was performed by standard methods,[48] and CIF files are available as Supplementary Material.

Synthetic Procedure A: Preparation of (IPr)CuFeCp(CO)(PR$_3$) (R= PEt$_3$, P^{n}Bu$_3$, PMe$_2$Ph, PMePh$_2$) (1a-d) and (IPr)Cu(μ-H)$_2$FeCp(PPh$_3$) (2). In a nitrogen filled glovebox, CpFe(CO)(PR$_3$)H (1 equiv.) was dissolved in C_6H_6 (1 mL) and kept the vial in freezer for 10 mins. In a separate vial, (IPr)CuOtBu (1 equiv.) was dissolved in C_6H_6. While stirring, (EtO)$_3$SiH (1.01 equiv.) was syringed in, turning the solution to a bright yellow color consistent with formation of [(IPr)CuH]$_2$. The [(IPr)CuH]$_2$ solution was pipette-filtered through Celite into the CpFe(CO)(PEt$_3$)H vial. The reaction turned orange brown in 5 mins and then the solution was dried *in vacuo*, resulting in an orange-brown precipitate. The solution was extracted with pentane and pipette-filtered through Celite. Crystallization was accomplished by leaving a concentrated solution in pentane at −35 °C.

Preparation of (IPr)CuFeCp(CO)(PEt$_3$) (1a). Following procedure A with CpFe(CO)(PEt$_3$)H (14.0 mg, 0.0522 mmol) in C_6H_6 (1 mL), (IPr)CuOtBu (27.4 mg, 0.0522 mmol) in C_6H_6 (1 mL), and (EtO)$_3$SiH (10.1 μL, 0.0530 mmol) Yield: 17.2 mg, 0.023 mmol, 44%. ^{1}H NMR (400 MHz, C_6D_6): δ 7.25 (t, J = 8.0 Hz, 2H, *p*-H), 7.12-7.18 (m, 4H, *m*-H), 6.30 (s, 2H, NCH), 4.01 (s, 5H, Cp), 2.92 (sept., J = 8.0 Hz, 2H, C<u>H</u>(CH$_3$)$_2$), 2.80 (sept., J = 8.0 Hz, 2H, C<u>H</u>(CH$_3$)$_2$), 1.50 (d, J = 12.0 Hz, 6H, CH(C<u>H$_3$</u>)$_2$), 1.49 (d, J = 12.0 Hz, 6H, CH(C<u>H$_3$</u>)$_2$), 1.38-1.45 (m, 3H, PC<u>H$_2$</u>CH$_3$), 1.09-1.16 (m, 3H, PC<u>H$_2$</u>CH$_3$), 1.09 (d, J = 8.0 Hz, 6H, CH(C<u>H$_3$</u>)$_2$), 1.08 (d, J = 8.0 Hz, 6H, CH(C<u>H$_3$</u>)$_2$), 0.88-0.97 (m, 9H, PCH$_2$C<u>H$_3$</u>). ^{31}P{^{1}H} NMR (162 MHz, C_6D_6): δ 68.49. ^{13}C{^{1}H} NMR (100 MHz, C_6D_6): δ 221.6 (CO), 179.6 (NCCu), 145.8, 136.0, 130.0, 124.0, 123.8, 121.2, 73.4 (Cp), 28.8, 28.7, 25.2, 25.0, 24.3, 24.2, 23.8, 23.6, 8.7. IR (solid, cm^{-1}): 2961, 2927, 2869, 1791 (ν_{CO}), 1457, 1401, 1326, 1180, 1104, 1003, 943, 799, 758, 730, 680, 533. Satisfactory elemental analysis data was not obtained due to thermal instability of the complex.

Preparation of (IPr)CuFeCp(CO)(P^{n}Bu$_3$) (1b). Following procedure A with CpFe(CO)(P^{n}Bu$_3$)H (25.0 mg, 0.0709 mmol) in C_6H_6 (1 mL), (IPr)CuOtBu (37.2 mg, 0.0709

mmol) in C_6H_6 (1 mL), and $(EtO)_3SiH$ (13.9 μL, 0.0710 mmol). Yield: 23.9 mg, 0.0297 mmol, 42%. ^1H NMR (400 MHz, C_6D_6): δ 7.27 (t, J = 8.0 Hz, 2H, *p*-H), 7.14-7.20 (m, 4H, *m*-H partial overlap with solvent peak), 6.27 (s, 2H, NCH), 4.00 (s, 5H, Cp), 2.95 (sept., J = 8.0 Hz, 2H, C<u>H</u>$(CH_3)_2$), 2.79 (sept., J = 8.0 Hz, 2H, C<u>H</u>$(CH_3)_2$), 1.53 (d, J = 8.0 Hz, 6H, CH(C<u>H</u>$_3)_2$), 1.51 (d, J = 16.0 Hz, 6H, CH(C<u>H</u>$_3)_2$), 1.19-1.46 (m, 18H, P(C<u>H</u>$_2)_3CH_3$), 1.10 (d, J = 8.0 Hz, 6H, CH(C<u>H</u>$_3)_2$), 1.10 (d, J = 8.0 Hz, 6H, CH(C<u>H</u>$_3)_2$), 0.96 (t, J = 8.0 Hz, 9H, P$(CH_2)_3$C<u>H</u>$_3$) . $^{31}P\{^1H\}$ NMR (162 MHz, C_6D_6): δ 61.53. $^{13}C\{^1H\}$ NMR (100 MHz, C_6D_6): δ 221.7 (CO), 179.6 (NCCu), 145.8, 136.1, 130.1, 124.1, 123.8, 121.2, 73.4 (Cp), 33.2, 33.0, 28.8, 28.7, 26.8, 24.8, 24.7, 24.2, 24.1, 24.0, 23.7, 14.0. IR (solid, cm^{-1}): 2960, 2925, 2866, 1795 (ν_{CO}), 1458, 1406, 1325, 1172, 1109, 946, 936, 801, 757, 733, 708, 573, 535. Satisfactory elemental analysis data was not obtained due to thermal instability of the complex.

Preparation of (IPr)CuFeCp(CO)(PMe$_2$Ph) (1c). Following procedure A with CpFe(CO)(P Me$_2$Ph)H (11.3 mg, 0.0392 mmol) in C_6H_6 (1 mL), (IPr)CuOtBu (20.5 mg, 0.0392 mmol) in C_6H_6 (1 mL), and $(EtO)_3SiH$ (7.7 μL, 0.0400 mmol). Yield: 6.7 mg, 0.009 mmol, 23%. ^1H NMR (400 MHz, C_6D_6): δ 7.81-7.85 (m, 2H, PC$_6$<u>H</u>$_6$), δ 7.22 (t, J = 8.0 Hz, 2H, *p*-H), 7.13-7.16 (m, 4H, *m*-H partial overlap with solvent peak), δ 7.11-7.13 (m, 2H, PC$_6$<u>H</u>$_6$), δ 7.03-7.06 (m, 1H, PC$_6$<u>H</u>$_6$), 6.31 (s, 2H, NCH), 3.93 (s, 5H, Cp), 2.87 (sept., J = 8.0 Hz, 2H, C<u>H</u>$(CH_3)_2$), 2.80 (sept., J = 8.0 Hz, 2H, C<u>H</u>$(CH_3)_2$), 1.53 (d, J = 8.0 Hz, 6H, CH(C<u>H</u>$_3)_2$), 1.49 (d, J = 8.0 Hz, 6H, CH(C<u>H</u>$_3)_2$), 1.41 (d, J = 8.0 Hz, 3H, PC<u>H</u>$_3$), 1.18 (d, J = 8.0 Hz, 3H, PC<u>H</u>$_3$), 1.10 (d, J = 8.0 Hz, 12H, CH(C<u>H</u>$_3)_2$). $^{31}P\{^1H\}$ NMR (400 MHz, C_6D_6): δ 44.89. IR (solid, cm^{-1}): 2961, 2927, 2868, 1793 (ν_{CO}), 1458, 1401, 1325, 1270, 1179, 1060, 1011, 932, 896, 799, 758, 741, 692, 599, 536. Satisfactory elemental analysis data was not obtained due to thermal instability of the complex.

Preparation of (IPr)CuFeCp(CO)(PMePh$_2$) (1d). Following procedure A with CpFe(CO)(PMePh$_2$)H (66.6 mg, 0.1903 mmol) in C_6H_6 (1 mL), (IPr)CuOtBu (100.0 mg, 0.1903 mmol) in C_6H_6 (1 mL), and $(EtO)_3SiH$ (38 μL, 0.1910 mmol). Yield: 32.1 mg, 0.039 mmol, 21%. ^1H NMR (400 MHz, C_6D_6): δ 7.75-7.79 (m, 2H, PC$_6$<u>H</u>$_6$), δ 7.54-7.58 (m, 2H, PC$_6$<u>H</u>$_6$), δ 7.22 (t, J = 8.0 Hz, 2H, *p*-H), 7.12-7.16 (m, 4H, *m*-H partial overlap with solvent peak), δ 7.07-7.10 (m, 6H, PC$_6$<u>H</u>$_6$), 6.31 (s, 2H, NCH), 3.93 (s, 5H, Cp), 2.93 (sept., J = 8.0 Hz, 2H, C<u>H</u>$(CH_3)_2$), 2.75 (sept., J = 8.0 Hz, 2H, C<u>H</u>$(CH_3)_2$), 1.51 (d, J = 4.0 Hz, 6H, CH(C<u>H</u>$_3)_2$), 1.44 (d, J = 8.0 Hz, 3H, PC<u>H</u>$_3$), 1.35 (d, J = 8.0 Hz, 6H, CH(C<u>H</u>$_3)_2$), 1.09 (d, J = 4.0 Hz, 6H, CH(C<u>H</u>$_3)_2$), 1.08 (d, J = 4.0 Hz, 6H, CH(C<u>H</u>$_3)_2$). $^{31}P\{^1H\}$ NMR (162 MHz, C_6D_6): δ 65.56. IR (solid, cm^{-1}): 2959, 2924, 2865, 1813 (ν_{CO}), 1457, 1433, 1325, 1211, 1085, 1064, 1011, 945, 879, 802, 759, 744, 698, 596, 538, 506. Satisfactory elemental analysis data was not obtained due to thermal instability of the complex.

Preparation of (IPr)Cu(μ-H)$_2$FeCp(PPh$_3$) (2). Following procedure A with CpFe(CO)(PPh$_3$)H (24.3 mg, 0.0587 mmol) in C_6H_6 (1 mL), (IPr)CuOtBu (31.0 mg, 0.0587 mmol) in C_6H_6 (1 mL), and $(EtO)_3SiH$ (11.8 μL, 0.0600 mmol. During recrystallization it was found that the decomposition product **2** was produced. Yield: 4.3 mg, 0.005 mmol, 9%. ^1H NMR (400 MHz, C_6D_6): δ 7.70-7.75 (m, 6H, PC$_6$<u>H</u>$_6$), δ 7.22 (m, 2H, *o*-H partial overlap with solvent peak), 7.09 (d, J = 8.0 Hz, 4H, *m*-H), δ 6.93-7.01 (m, 9H, PC$_6$<u>H</u>$_6$), 6.19 (s, 2H, NCH), 3.66 (s, 5H, Cp), 2.77 (sept., J = 8.0 Hz, 4H, C<u>H</u>$(CH_3)_2$), C<u>H</u>$(CH_3)_2$), 1.42 (d, J = 8.0 Hz, 12H, CH(C<u>H</u>$_3)_2$), 1.09 (d, J = 8.0 Hz, 12H, CH(C<u>H</u>$_3)_2$), -17.77 (d, J = 40.0 Hz, 2H, μ-<u>H</u>). $^{31}P\{^1H\}$ NMR (162 MHz, C_6D_6): δ 94.69. IR (solid, cm^{-1}): 2958, 2924, 2867, 1616, 1585, 1471, 1433, 1309, 1268, 1181, 1062, 1000, 988, 942, 803, 745, 694, 530, 516, 496, 474, 449, 422.

Procedure B: Preparation of (NHC)CuWCp*(CO)$_2$(PR$_3$) (3a-c). Cp*W(CO)$_2$(PR$_3$)H was produced by the addition of phosphine (3 equiv.) to a solution of Cp*W(CO)$_3$H (1.5 equiv.) in toluene (10 mL) and heating at 110°C in a closed vial for three days. The crude product was pumped down *in vacuo* at room temperature until dry and then at 60°C for 3 h. The crude material was then dissolved in pentane (10 mL) and stored at -30°C overnight. The solution was pipet-filtered through Celite to remove white crystals and used without further purification. In a separate vial, (NHC)CuOtBu (1 equiv.) was dissolved in pentane (5 mL). While stirring, (EtO)$_3$SiH (1 equiv.) was syringed in, turning the solution to a bright yellow color consistent with formation of [(IPr)CuH]$_2$. The [(IPr)CuH]$_2$ solution was pipette-filtered through Celite into the solution of Cp*W(CO)$_2$(PR$_3$)H. The reaction was left to stir overnight with slow formation of a dark yellow-orange color. The crude product was recrystallized two times from slow evaporation of pentane solutions in the glovebox freezer at -30°C to obtain yellow to red crystals suitable for characterization.

Preparation of IPrCuWCp*(CO)$_2$(PEt$_3$) (3a). Following procedure B, PEt$_3$, (37.6 mg, 0.495 mmol), Cp*W(CO)$_3$H (100mg, 0.247 mmol), (IPr)CuOtBu (89 mg, 0.17 mmol), and (EtO)$_3$SiH (25 µL, 0.17 mmol) were used. Yield: 105 mg, 0.11 mmol, 66%. ^{1}H NMR (400 MHz, C_6D_6): δ 7.36-7.16 (m, 3H, ArH), 6.41 (s, 2H, NCH), 2.97 (sept., J = 6.5 Hz, 4H, C<u>H</u>(CH$_3$)$_2$), 1.96 (s, 15H, Cp*), 1.58 (d, J = 6.5 Hz, 12 H, CH(C<u>H$_3$</u>)$_2$), 1.36 (t, J = 8.0 Hz, 9H, PCH$_2$C<u>H$_3$</u>), 1.08 (d, J = 6.5 Hz, 12H, CH(C<u>H$_3$</u>)$_2$), 1.01-0.94(m, 6H, PC<u>H$_2$CH$_3$</u>) ^{31}P{^{1}H} NMR (162 MHz, C_6D_6): δ 21.24. IR (solid, cm^{-1}): 2957, 2869, 1750(ν_{CO}), 1691(ν_{CO}), 1456, 1364, 1330, 1027, 802, 759, 700, 564, 483, 418. Elemental analysis calculated (%) for [$C_{45}H_{62}O_2CuWPN_2$] C 57.41, H 6.63, N 2.97; found C 57.39, H 6.88, N 2.92.

Preparation of IPrCuWCp*(CO)$_2$(PMe$_2$Ph) (3b). Following procedure B, PMe$_2$Ph, (68.38 mg, 0.495 mmol), Cp*W(CO)$_3$H (100mg, 0.247 mmol), (IPr)CuOtBu (89 mg, 0.17 mmol), and (EtO)$_3$SiH (25 µL, 0.17 mmol) were used. Yield: 96 mg, 0.10 mmol, 60%. ^{1}H NMR (400 MHz, C_6D_6): δ 7.72 (t, J = 7.5 Hz, 2H, ArH), 7.26-7.22 (m, 3H, ArH), 7.16-7.13 (m, 2H, ArH-overlap with solvent) 7.03-6.96 (m, 4H, ArH), 6.45 (s, 2H, NCH), 2.97 (sept., J = 6.5 Hz, 4H, C<u>H</u>(CH$_3$)$_2$), 1.80 (s, 15H, Cp*), 1.61 (d, J = 6.5 Hz, 12 H, CH(C<u>H$_3$</u>)$_2$), 1.52 (s, 3H, PMe), 1.50 (s, 3H, PMe), 1.10 (d, J = 6.5 Hz, 12H, CH(C<u>H$_3$</u>)$_2$), ^{31}P{^{1}H} NMR (162 MHz, C_6D_6): δ 3.35. IR (solid, cm^{-1}): 3114, 2960, 2906, 2866, 1778(ν_{CO}), 1702(ν_{CO}), 902, 800, 743, 698, 677, 573, 483, 427. Repeated attempts at elemental analysis did not give satisfactory results. ^{1}H and ^{31}P NMR spectroscopy was used to assess purity (see Supplementary Material).

Preparation of IPrCuWCp*(CO)$_2$(PMePh$_2$) (3c). Following procedure B, PMePh$_2$, (99.1 mg, 0.495 mmol), Cp*W(CO)$_3$H (100mg, 0.247 mmol), (IPr)CuOtBu (89 mg, 0.17 mmol), and (EtO)$_3$SiH (25 µL, 0.17 mmol) were used. Yield: 75 mg, 0.073 mmol, 43%. ^{1}H NMR (400 MHz, C_6D_6): δ 7.72 (t, J = 7.5 Hz, 4H, ArH), 7.24-7.12 (m, 10H, ArH), 7.03 (t, J = 7.0 Hz, 2H, ArH) 6.42 (s, 2H, NCH), 2.94 (sept., J = 7.0 Hz, 4H, C<u>H</u>(CH$_3$)$_2$), 1.78 (s, 15H, Cp*), 1.75 (d, J = 8.1 Hz, 3H, PMe) 1.53 (d, J = 7.0 Hz, CH(C<u>H$_3$</u>)$_2$), 1.07 (d, J = 7.0 Hz, 12H, CH(C<u>H$_3$</u>)$_2$), ^{31}P{^{1}H} NMR (162 MHz, C_6D_6): δ 25.64. IR (solid, cm^{-1}): 2962, 2901, 2867, 1762(ν_{CO}), 1693(ν_{CO}), 1459, 887, 744, 695, 524, 490, 422. Elemental analysis calculated (%) for [$C_{52}H_{60}O_2CuWPN_2$] C 61.03, H 5.91, N 2.74; found C 60.87, H 5.91, N 2.59.

Preparation of 6PrCuWCp*(CO)$_2$(PEt$_3$) (3d). PEt$_3$, (32 mg, 0.420 mmol, 2 equiv.) was added to a solution of Cp*W(CO)$_3$H (85 mg, 0.210, 1.5 equiv.) in toluene (10 mL) and heated at 110°C for three days. The crude product was pumped down *in vacuo* at room temperature until dry and then at 60°C for 3 h to give 104 mg (0.210mmol. The crude product was dissolved pentane (10 mL), and 6PrCuH (98 mg, 0.21 mmol) was added. Recrystallization from slow

evaporating pentane in the glovebox freezer at -30°C gave pure product. This product was further recrystallized in slow evaporating pentane to afford crystals for single crystal XRD analysis. Yield: 30 mg, 0.031 mmol, 15%. ^{1}H NMR (400 MHz, C_6D_6): δ 7.24-7.17 (m, 4H, Ar-H significant overlap with solvent), 3.41 (sept., J = 6.7 Hz, 4H, C<u>H</u>$(CH_3)_2$), 2.92 (t, J = 5.7 Hz, 4H, NC<u>H$_2$</u>CH_2C<u>H$_2$</u>N) 1.88 (s, 15H, Cp*), 1.74 (d, J = 6.5 Hz, 12 H, CH(C<u>H$_3$</u>)$_2$), 1.17 (d, J = 6.5 Hz, 12H, CH(C<u>H$_3$</u>)$_2$), 1.01-0.94 (m, 9H, PCH_2C<u>H$_3$</u>), 0.89-0.80(m, 6H, PC<u>H$_2$</u>CH_3) ^{31}P{^{1}H} NMR (162 MHz, C_6D_6): δ 20.75. IR (solid, cm−1): 2956, 2930, 2902, 2872, 1753(ν_{CO}), 1688, 1483, 1446, 1321, 1295, 1198, 1026, 803, 758, 700, 641, 604, 560, 410. *m*/*z* (APCI+ SIM mode): 118.1(PEt_3), 135.2(Cp*), 404.3(6Pr), 467.2(6PrCu), 493.1(Cp*W$(CO)_2PEt_3$), 960.4(6PrCuCp*W$(CO)_2PEt_3$)

Acknowledgements: Funding was provided by the National Science Foundation (CHE-1664632). Dr. Chia-Wei Hsu assisted with mass spectrometric analysis.

References

[1] J.F. Hartwig, Evolution of C-H Bond Functionalization from Methane to Methodology., J. Am. Chem. Soc. 138 (2016) 2–24. doi:10.1021/jacs.5b08707.

[2] H.M.L. Davies, J. Du Bois, J.-Q. Yu, C–H Functionalization in organic synthesis, Chem. Soc. Rev. 40 (2011) 1855. doi:10.1039/c1cs90010b.

[3] K.M. Engle, T.-S. Mei, M. Wasa, J.-Q. Yu, Weak Coordination as a Powerful Means for Developing Broadly Useful C–H Functionalization Reactions, Acc. Chem. Res. 45 (2012) 788–802. doi:10.1021/ar200185g.

[4] W.R. Gutekunst, P.S. Baran, C–H functionalization logic in total synthesis, Chem. Soc. Rev. 40 (2011) 1976. doi:10.1039/c0cs00182a.

[5] W.D. Jones, F.J. Feher, Comparative reactivities of hydrocarbon carbon-hydrogen bonds with a transition-metal complex, Acc. Chem. Res. 22 (1989) 91–100. doi:10.1021/ar00159a002.

[6] W.D. Jones, Enhanced: Conquering the Carbon-Hydrogen Bond, Science. 287 (2000) 1942–1943. doi:10.1126/science.287.5460.1942.

[7] I.A.I. Mkhalid, J.H. Barnard, T.B. Marder, J.M. Murphy, J.F. Hartwig, C−H Activation for the Construction of C−B Bonds, Chem. Rev. 110 (2010) 890–931. doi:10.1021/cr900206p.

[8] J.-Y. Cho, M.K. Tse, D. Holmes, R.E. Maleczka, M.R. Smith, Remarkably selective iridium catalysts for the elaboration of aromatic C-H bonds., Science. 295 (2002) 305–308. doi:10.1126/science.1067074.

[9] J.F. Hartwig, Borylation and Silylation of C–H Bonds: A Platform for Diverse C–H Bond Functionalizations, Acc. Chem. Res. 45 (2012) 864–873. doi:10.1021/ar200206a.

[10] Y. Ohki, T. Hatanaka, K. Tatsumi, C−H Bond Activation of Heteroarenes Mediated by a Half-Sandwich Iron Complex of N-Heterocyclic Carbene, J. Am. Chem. Soc. 130 (2008) 17174–17186. doi:10.1021/ja8063028.

[11] T. Hatanaka, Y. Ohki, K. Tatsumi, CH Bond Activation/Borylation of Furans and Thiophenes Catalyzed by a Half-Sandwich Iron N-Heterocyclic Carbene Complex, Chem. - An Asian J. 5 (2010) 1657–1666. doi:10.1002/asia.201000140.

[12] Y. Yoshigoe, Y. Kuninobu, Iron-Catalyzed *ortho* -Selective C–H Borylation of 2-

Phenylpyridines and Their Analogs, Org. Lett. 19 (2017) 3450–3453. doi:10.1021/acs.orglett.7b01423.
[13] T. Furukawa, M. Tobisu, N. Chatani, Nickel-catalyzed borylation of arenes and indoles via C-H bond cleavage., Chem Commun. 51 (2015) 6508–6511. doi:10.1039/c5cc01378j.
[14] J. V Obligacion, S.P. Semproni, P.J. Chirik, Cobalt-Catalyzed C–H Borylation, J. Am. Chem. Soc. 136 (2014) 4133–4136. doi:10.1021/ja500712z.
[15] J. V Obligacion, S.P. Semproni, I. Pappas, P.J. Chirik, Cobalt-Catalyzed C(sp 2)-H Borylation: Mechanistic Insights Inspire Catalyst Design, J. Am. Chem. Soc. 138 (2016) 10645–10653. doi:10.1021/jacs.6b06144.
[16] J. V. Obligacion, P.J. Chirik, Mechanistic Studies of Cobalt-Catalyzed C(sp^2)–H Borylation of Five-Membered Heteroarenes with Pinacolborane, ACS Catal. 7 (2017) 4366–4371. doi:10.1021/acscatal.7b01151.
[17] C.R.K. Jayasundara, D. Sabasovs, R.J. Staples, J. Oppenheimer, M.R. Smith, R.E. Maleczka, Cobalt-Catalyzed C–H Borylation of Alkyl Arenes and Heteroarenes Including the First Selective Borylations of Secondary Benzylic C–H Bonds, Organometallics. 37 (2018) 1567–1574. doi:10.1021/acs.organomet.8b00144.
[18] J. V. Obligacion, H. Zhong, P.J. Chirik, Insights into Activation of Cobalt Pre-Catalysts for C(sp^2)−H Functionalization, Isr. J. Chem. 57 (2017) 1032–1036. doi:10.1002/ijch.201700072.
[19] M.-A. Légaré, M.-A. Courtemanche, É. Rochette, F.-G. Fontaine, Metal-free catalytic C-H bond activation and borylation of heteroarenes., Science. 349 (2015) 513–516. doi:10.1126/science.aab3591.
[20] R.H. Morris, Brønsted–Lowry Acid Strength of Metal Hydride and Dihydrogen Complexes, Chem. Rev. 116 (2016) 8588–8654. doi:10.1021/acs.chemrev.5b00695.
[21] N.P. Mankad, Diverse bimetallic mechanisms emerging from transition metal Lewis acid/base pairs: development of co-catalysis with metal carbenes and metal carbonyl anions., Chem Commun. 34 (2018) 5497. doi:10.1039/c7cc09675e.
[22] M.K. Karunananda, N.P. Mankad, E-Selective Semi-Hydrogenation of Alkynes by Heterobimetallic Catalysis., J. Am. Chem. Soc. 137 (2015) 14598–14601. doi:10.1021/jacs.5b10357.
[23] S. Bagherzadeh, N.P. Mankad, Catalyst Control of Selectivity in CO 2Reduction Using a Tunable Heterobimetallic Effect, J. Am. Chem. Soc. 137 (2015) 10898–10901. doi:10.1021/jacs.5b05692.
[24] T.J. Mazzacano, N.P. Mankad, Base Metal Catalysts for Photochemical C–H Borylation That Utilize Metal–Metal Cooperativity, J. Am. Chem. Soc. 135 (2013) 17258–17261. doi:10.1021/ja408861p.
[25] T.J. Mazzacano, New Developments in Base Metal-Catalyzed C-H Borylation, Ph.D. thesis, University of Illinois at Chicago, 2017.
[26] K.M. Waltz, X. He, C. Muhoro, J.F. Hartwig, Hydrocarbon functionalization by transition metal boryls, J. Am. Chem. Soc. 117 (1995) 11357–11358.
[27] K.M. Waltz, C.N. Muhoro, J.F. Hartwig, C−H Activation and Functionalization of Unsaturated Hydrocarbons by Transition-Metal Boryl Complexes, Organometallics. 18 (1999) 3383–3393. doi:10.1021/om990113v.
[28] K.M. Waltz, J.F. Hartwig, Functionalization of Alkanes by Isolated Transition Metal Boryl Complexes, J. Am. Chem. Soc. 122 (2000) 11358–11369. doi:10.1021/ja002840j.
[29] S.R. Parmelee, T.J. Mazzacano, Y. Zhu, N.P. Mankad, J.A. Keith, A Heterobimetallic

Mechanism for C–H Borylation Elucidated from Experimental and Computational Data, ACS Catal. 5 (2015) 3689–3699. doi:10.1021/acscatal.5b00275.
[30] K.R. Sawyer, J.F. Cahoon, J.E. Shanoski, E.A. Glascoe, M.F. Kling, J.P. Schlegel, M.C. Zoerb, M. Hapke, J.F. Hartwig, C.E. Webster, C.B. Harris, Time-resolved IR Studies on the Mechanism for the Functionalization of Primary C−H Bonds by Photoactivated Cp*W(CO) 3(Bpin), J. Am. Chem. Soc. 132 (2010) 1848–1859. doi:10.1021/ja906438a.
[31] N. Mankad, Non-Precious Metal Catalysts for C–H Borylation Enabled by Metal–Metal Cooperativity, Synlett. 25 (2014) 1197–1201. doi:10.1055/s-0033-1340823.
[32] T.J. Mazzacano, N.P. Mankad, Thermal C-H borylation using a CO-free iron boryl complex, Chem Commun. 51 (2015) 5379–5382. doi:10.1039/C4CC09180A.
[33] M.K. Karunananda, N.P. Mankad, Heterobimetallic H 2Addition and Alkene/Alkane Elimination Reactions Related to the Mechanism of E-Selective Alkyne Semihydrogenation, Organometallics. 36 (2017) 220–227. doi:10.1021/acs.organomet.6b00356.
[34] U. Jayarathne, T.J. Mazzacano, S. Bagherzadeh, N.P. Mankad, Heterobimetallic Complexes with Polar, Unsupported Cu–Fe and Zn–Fe Bonds Stabilized by N-Heterocyclic Carbenes, Organometallics. 32 (2013) 3986–3992. doi:10.1021/om400471u.
[35] S. Banerjee, M.K. Karunananda, S. Bagherzadeh, U. Jayarathne, S.R. Parmelee, G.W. Waldhart, N.P. Mankad, Synthesis and Characterization of Heterobimetallic Complexes with Direct Cu–M Bonds (M = Cr, Mn, Co, Mo, Ru, W) Supported by N-Heterocyclic Carbene Ligands: A Toolkit for Catalytic Reaction Discovery, Inorg. Chem. 53 (2014) 11307–11315. doi:10.1021/ic5019778.
[36] F.A. Cotton, L.M. Daniels, C.A. Murillo, H.C. Zhou, The effect of divergent-bite ligands on metal–metal bond distances in some paddlewheel complexes, Inorganica Chim. Acta. 300–302 (2000) 319–327. doi:10.1016/S0020-1693(99)00537-X.
[37] S.R. Parmelee, N.P. Mankad, A data-intensive re-evaluation of semibridging carbonyl ligands, Dalt. Trans. 44 (2015) 17007–17014. doi:10.1039/C5DT02813B.
[38] M.D. Curtis, K.R. Han, W.M. Butler, Metal-metal multiple bonds. 5. Molecular structure and fluxional behavior of tetraethylammonium. mu.-cyano-bis (cyclopentadienyldicarbonylmolybdate)(Mo-Mo) and the question of semibridging carbonyls, Inorg. Chem. 19 (1980) 2096–2101.
[39] M.K. Karunananda, F.X. Vázquez, E.E. Alp, W. Bi, S. Chattopadhyay, T. Shibata, N.P. Mankad, Experimental determination of redox cooperativity and electronic structures in catalytically active Cu–Fe and Zn–Fe heterobimetallic complexes, Dalt. Trans. 43 (2014) 13661. doi:10.1039/C4DT01841A.
[40] A. Hicken, A.J.P. White, M.R. Crimmin, Preparation and characterisation of heterobimetallic copper–tungsten hydride complexes, Dalt. Trans. 47 (2018) 10595-10600. doi:10.1039/C8DT01569D.
[41] G.J. Kubas, Dihydrogen complexes as prototypes for the coordination chemistry of saturated molecules., Proc. Natl. Acad. Sci. U. S. A. 104 (2007) 6901–7. doi:10.1073/pnas.0609707104.
[42] Azwana R. Sadique, Elizabeth A. Gregory, and William W. Brennessel, P.L. Holland*, Mechanistic Insight into NN Cleavage by a Low-Coordinate Iron(II) Hydride Complex, (2007). doi:10.1021/JA069199R.
[43] R.H. Morris, Estimating the acidity of transition metal hydride and dihydrogen complexes by adding ligand acidity constants., J. Am. Chem. Soc. 136 (2014) 1948–1959.

doi:10.1021/ja410718r.
[44] N.P. Mankad, D.S. Laitar, J.P. Sadighi, Synthesis, Structure, and Alkyne Reactivity of a Dimeric (Carbene)copper(I) Hydride, Organometallics. 23 (2004) 3369–3371. doi:10.1021/om0496380.
[45] A.J. Jordan, C.M. Wyss, J. Bacsa, J.P. Sadighi, Synthesis and Reactivity of New Copper(I) Hydride Dimers, Organometallics. 35 (2016) 613–616. doi:10.1021/acs.organomet.6b00025.
[46] D. A. Brown, H.J. Lyons, A.R. Manning, A new type of isomerism in some phosphine and phosphite derivatives of the metal carbonyls, Inorganica Chim. Acta. 4 (1970) 428–430. doi:10.1016/S0020-1693(00)93320-6.
[47] H.G. Alt, H.E. Engelhardt, W. Kläui, A. Müller, Trimethylphosphan- und Carbonyl-hydrid-Halbsandwichkomplexe des Chroms, Molybdäns und Wolframs: C5Hf5−, C5Me5− und ein isoelektronischer 6e−-Sauerstof-Tripodligand im Vergleich, J. Organomet. Chem. 331 (1987) 317–327. doi:10.1016/0022-328X(87)80004-9.
[48] P. Müller, Practical suggestions for better crystal structures, Crystallogr. Rev. 15 (2009) 57–83. doi:10.1080/08893110802547240.